RSC Advances

ROYAL SOCIETY OF CHEMISTRY

www.rsc.org/advances

Synthesis of novel glycerol based B_3-type monomer and its application in Hyperbranched polyester urethane-urea coatings

Somisetti Varaprasad, Shaik Allauddin, Ramanuj Narayan and KVSN Raju*

Polymers & Functional Materials Division, Indian Institute of Chemical Technology, Hyderabad-500007, India

Glycerol (GLY) based hyperbranched polyester polyols (HBP) were synthesized by the reaction of GLY and Succinic anhydride (SA) as a B_3-type monomer with GLY as the core moiety without using any solvent. Acid terminated B_3 monomer and HBP were characterized by techniques such as ^1H, and ^{13}C nuclear magnetic resonance spectroscopy (NMR), Fourier transform infrared (FTIR) spectroscopy, gel permeation chromatography (GPC), differential scanning calorimetry (DSC), and thermogravimetric analysis (TGA). Degree of branching present in the HBP was calculated by NMR spectroscopy. The HBP was further reacted with different ratios of isophorone diisocyanate (IPDI) to get isocyanate-terminated polyurethane prepolymer that was cured under atmospheric moisture to get the desired coating films. Thermo-mechanical, viscoelastic and contact angle properties of these films were also evaluated. Glass transition temperatures (T_g) of the cross-linked networks were found to be in the range of 95−125 ^oC, and the water contact angles were in the range of 78^o−82^o. The T_g and hydrophobic character of the coating films found to increase with an increasing NCO:OH ratio. This work provides an effective and promising way to prepare glycerol based HBPs for high-performance coatings.

Keywords: Glycerol, degree of branching, glass transition, polyester, thermal

**Correspondence to*: K.V.S.N.Raju (E-mail: kvsnraju@iict.res.in drkvsnraju@gmail.com), fax: +91-40-27193991

1. INTRODUCTION

In recent years, the sustainability is becoming increasingly important for the chemical industry thus, Polymers from renewable resources are gaining a lot of interest, especially with the high price and limited availability of crude oil. Our research group has explored the direct utilization of glycerol to produce HBPs.[1-3] Owing to the use of glycerol, making polymers from it would be an efficient utilization for coating industry because glycerol is the principle coproduct in the transesterification process by which biodiesel is produced.[4] HBPs have received increased attention recently because of their low viscosity and a highly branched architecture can be produced at low cost for large scale application with a wide range of physical and chemical properties [5-6] and these can be prepared with commercially available raw materials. Hence, HBPs gained much attention of the research communities and industries in the area of developing coatings, additives, sealants, lubricants etc.[7-8] Polyurethanes (PUs) are a class of polymers with unique and versatile chemistry which have wide range of applications[9] Most importantly, hyperbranched polyurethanes (HBPUs) have been used in coating industries due to their low melting viscosities, good solubility in different solvents, high density of functional terminal groups and their high glass transition temperatures.[10]

The most common synthesis of hyperbranched (HB) polymers in single monomer methodology is the intermolecular polymerization of AB_2 strategies[11-12] where A and B represent different functional group monomers intermolecularly polymerized to build up HB structures, However, AB_2 monomers are expensive and have to be synthesized prior to the polymerization step.[13] An alternative method to build up HBP was proposed by Flory[14] in which he described the critical gel point for AB_2 HBP produced from AB_2 monomers. Apart from this AB_2 polymerization, another route A_2+B_3 was proposed by Flory et al. for the first time which comes

under double monomer methodology (DMM) then followed by development of HBP through this process.[15-18]

As there are many limitations like commercial unavailability of monomers, gelation, solubility and uncontrollable molecular weight, a new synthetic method was established namely couple monomer methodology (CMM). This methodology developed by Yan and Gao[19-21] , which involves strategies like A_2+BB_2^*, A_2+CB_2, AB+CD_n, A^*+B_n and AA^*B_2 . The A_3+B_3 type approach adopted in the synthesis of HBP is somewhat less explored, which gives complete symmetry to the monomers and provides better chances of maximized formation of HBP without gelation. In the present work, we wish to establish the potential for using glycerol as renewable resources, to replace petroleum based monomers (high price monomers). To this achievement, an acid terminated monomer (B_3) was synthesized by nucleophilic ring-opening addition reaction of GLY and SA, which was further reacted with GLY (A_3) monomer in a solvent-free one pot reaction to form HBP. Herein, we described the synthesis as well as thermal and mechanical properties, contact angle, and morphological properties of PU films based on HBP (Scheme 1). To develop a high-performance moisture curable coating composition, we successfully studied the effect of the NCO/OH ratio on HBP and also its effect on thermo-mechanical properties in moisture curable systems. Synthesized HBP was further reacted with isophorone diisocyanate (IPDI) at different NCO/OH equivalent ratios to get NCO-terminated prepolymers. The physical and thermal properties were studied using differential scanning calorimetry (DSC), thermogravimetric analysis (TGA), dynamic mechanical thermal analysis (DMTA), and XRD measurements. Our research efforts are focused on the development of a novel synthetic method for HBP, which can be a potential candidate for replacing or partially replacing petroleum-based PU coatings.

2. EXPERIMENTAL

2.1. Materials. Glycerol (GLY) was procured from Qualigens (India). Isophorone diisocyanate (IPDI, 98%), Succinic anhydride(SA, 99%) were supplied by Alfa Aesar (MA, USA). Tin (II) chloride ($SnCl_2$, ≥99.99%) and Dibutyltindilaurate (DBTDL, 95%) were obtained from Aldrich (Milwaukee, WI). All other chemicals were analytical grade and were used without further purification.

2.2. Synthesis of Acid terminated Hyperbranched Polyester (B_3). The Acid terminated hyperbranched polyester was synthesized, in a four-necked reaction flask by charging GLY and SA in a mole ratio of 1:3. Reaction was maintained at 120 ^oC in the presence of 1 wt% of $SnCl_2$ as a catalyst. It was monitored through FTIR spectroscopy by collecting product sample during the reaction time at regular intervals and stopped when the anhydride peak at 1850 cm^{-1} disappeared completely in the FTIR spectra. The acid value (A.V) of B_3-type monomer was measured according to the ASTM standard D 1639-89. Schematic representation for the synthesis of the B_3 is shown in Scheme 1.

B_3: ^{1}HNMR ($CDCl_3$, δ, ppm): 2.5-2.6 (C<u>H</u>2−COOH & C<u>H</u>2−COO−), 4.1-4.3 (−C<u>H</u>2−OCO−), 5.2 (−C<u>H</u>−O−CO−); ^{13}CNMR ($CDCl_3$, δ, ppm): 28.1 (−<u>C</u>H2−COOH & −<u>C</u>H2−COO−), 61.7 (−<u>C</u>H2−OCO−), 68.5 (−<u>C</u>H−O−CO−), 172.75 (−<u>C</u>OO−), 174.17 (−<u>C</u>OOH); FTIR (KBr, cm^{-1}):3,423 (s, OH str, −COOH), 1,732 (s, −C=O str), 1,162 (s, O=CO−C str), 1,069 1,026 (m, O=C−OH str).

2.3. Synthesis of hydroxyl terminated hyperbranched polyester (HBP). Hydroxyl terminated hyperbranched polyester was synthesized by charging B_3 and A_3 (GLY) in a mole ratio of 1:3 and reaction was continued at about 150-160 ^oC. The eliminated water was collected from the Dean-Stark apparatus. The reaction was monitored periodically by checking the acid

value through a simple titration method and stopped when the acid value was below five. The synthesized hydroxyl terminated polyester was named as HBP. Hydroxyl value of the synthesized HBP was measured according to the ASTM standard D 4274-94. The schematic representation for the synthesis of the HBP is shown in Scheme 1. The product was further characterized by FTIR and ^{1}H & ^{13}CNMR.

HBP: ^{1}HNMR ($CDCl_3$, δ, ppm): 2.6 (−C$\underline{H}_2$−COO−), 4.03 & 4.23 (−C$\underline{H}_2$−OCO−), 5.23 (−C$\underline{H}$−O−CO−), 3.39 & 3.54 (−C$\underline{H}_2$−OH), 3.69 & 3.92 (−C$\underline{H}$−OH). ^{13}CNMR ($CDCl_3$, δ, ppm): 28.1 (−$\underline{C}H_2$−COO−), 62.08 (−$\underline{C}$H2−OCO−), 69.09 (−$\underline{C}$H−O−CO−), 171.34-172.03 (−$\underline{C}$OO−), 62.88 & 59.75 (−$\underline{C}H_2$−OH), 66.16 & 69.43 (−$\underline{C}$H−OH). FTIR (KBr, cm^{-1}): 3,425 (s, −OH str), 2,931 and 2,895 (m, −CH2 str), 1,728 (s, C=O str), 1,029 (s, −C−OH str)

2.4. Synthesis of Polyurethane-Urea coating films. Coating films were prepared using the formulations which are summarized in Table 1. The synthesized HBP was further reacted with IPDI in presence of 0.01 wt % of DBTL as catalyst at different NCO:OH equivalent ratios (1.2:1, 1.4:1, 1.6:1 and 2:1) at around 70-80 ^{o}C to get different –NCO terminated prepolymers. Above prepared –NCO terminated hyperbranched PU prepolymers (HBPPU) were used further for the preparation of final coatings. The –NCO terminated prepolymer films were casted on tin foil supported on glass plate using manual driven square applicator. The films were kept in the open atmosphere, at the laboratory humidity condition for a period of 15 days to get moisture cured HBPPU-urea films. They were removed from the glass plate and the free films of the coatings were obtained by amalgamation technique. The disappearance of –NCO peak at 2270 cm^{-1} from FTIR spectroscopy was taken as a measure of complete cure. The different formulations and mole ratios are shown in Table 1 and the schematic representation for formation of poly (urethane-urea) has shown in Scheme 2.

3. CHARACTERIZATION

Characterization of polymers was done by gel permeation chromatography (GPC: C-R4A Chrotopac; Shimadzu, Kyoto, Japan), samples were dissolved in THF solvent by taking 0.1 g/10mL and experiments were carried out at a flow rate of 1.0mL/min using THF as the mobile phase. Columns were calibrated with Aldrich polystyrene standards. The structures of polymers and coating films were characterized by using Fourier-Transform Infrared Spectroscopy (FTIR) using Thermo Nicolet Nexus 670 spectrometer. Each sample was scanned 128 times with resolution, 4 cm^{-1} and averaged to obtain the spectrum. All the spectra were scanned within the range 400-4000 cm^{-1}. The ^{1}H & ^{13}C Nuclear Magnetic Resonance Spectroscopy (NMR) spectra were recorded in $CDCl_3$ solution using a Varian-Inova-500 MHz spectrometer. Chemical shifts (δ) are given in ppm with tetramethyl silane as a standard. Thermal analysis was done by a Dynamic Mechanical Thermal Analysis (DMTA) IV instrument (Rheometric Scientific, USA) in tensile mode at a frequency of 1 Hz with a heating rate of 3 ^{o}C/min by scanning the films from 27 ^{o}C to 200 ^{o}C. Storage modulus (E') and tan δ as a function of temperature at a constant frequency were observed. Chemical resistance of the films was studied using ASTM D543-67 (1972) method. Thermogravimetric analysis (TGA) measurements were performed on a TA Q500 (TA Instruments, Inc.) with a heating rate of 10 ^{o}C/min under a N_2 atmosphere. The weight of the samples was ranged from 5–10 mg. Differential scanning calorimetry (DSC) analysis was recorded on a Mettler Toledo DSC 821^{e}, Switzerland. Samples were heated from -70 ^{o}C to 150 ^{o}C at a heating rate of 10 ^{o}C/ min under nitrogen atmosphere at a flow rate of 30 mL/ min. The viscosity of polymers was determined by using Haake rotational viscometer 2.1 system M5/SV2 (HAAKE, Germany). Contact angle was measured by G10 (KRUSS) instrument through sessile drop method. Powder X-ray diffraction patterns (XRD) of coating films were recorded at

different diffraction angles (2θ) using Siemens/D-5000 diffractometer with CuKa radiation (l = 1.5406 Å).

4. RESULTS AND DISCUSSION

4.1. Characterization of B_3 and HBP. Fourier-transform infrared (FTIR) spectroscopy was used to follow the chemical structure of the polymers. The progress of the reaction between GLY and SA in presence of $SnCl_2$ catalyst at 120 ^oC was monitored by FTIR spectroscopy and the resulting final spectrum is shown in Figure 1. From the spectrum, we could observe the disappearance of anhydride peak between 1779-1850 cm^{-1} and appearances of the strong ester carbonyl peak at 1723 cm^{-1} which confirms the completion of the reaction. The presence of ester group is reconfirmed by appearance of a peak at 1280 cm^{-1}due to ─(CO)─O─C─ stretching mode and appearance of stretching C−O acid and C−O −C ester peak at 1727 and 1280cm^{-1} indicates the completion of the reaction between GLY and SA. The FTIR spectrum of the synthesized B_3 and HBP is shown in Figure 1. In HBP the broad peak at 3425 cm^{-1} and also a sharp peak at 1754 cm^{-1} are attributed to the −OH stretching absorbance and the −C=O group of the ester linkages.[22] The broad peak −OH stretching band at about 3425 cm^{-1} is due to the combined effect of the differently associated hydroxyl groups, i.e., intra/inter molecular hydrogen bonding between different −OH groups or between −OH and −C=O groups. The structures of B_3 and HBP were further supported by ^1H and ^{13}CNMR spectroscopy analyses. The ^1H and ^{13}CNMR spectra of both B_3 and HBP are shown in Figure 2 and Figure 3. Dendentric and hyperbranched units exhibited different chemical shift values based on their environment in both ^1H and ^{13}CNMR and the values are given in the Table 2. All these value are in consistent with the previous reports as well.[23-24] To correlate the units of HBP and describe the structure of HBP

quantitatively, Frechet and co-workers gave an equation for the Degree of branching (DB) at first, as shown in following Equation (1).

DB = (no. of dendritic units) + (no. of terminal units)/ total no. of units

$$DB = (D + T)/ (D + T + L) \quad (1)$$

Here, D is the total number of dendritic units, T the total number of terminal units, and L the total number of linear units. D are tri-substituted GLY units, while two different L units as di-esterified GLY monomers, either in a 1,2- ($L_{1,2}$) or a 1,3-connection ($L_{1,3}$), were to be expected. As far as T units are concerned, they can be of three different types, that is mono-substituted GLY, either with two primary ($T_{1,3}$) or one primary and one secondary OH-group ($T_{1,2}$), and carboxylic acid end groups (TA).[13] NMR spectroscopy, however, can determine how many GLY units have reacted and at which of the primary or secondary alcohol positions the diacids are located. Therefore, it can characterize the types of branching patterns and measure their relative occurrence. This information can be seen in Figure 4 and data summarized in Table 2, as a degree of branching ratio (DB %). The DB for HBP calculated according to equation (1) from ^{1}HNMR and ^{13}CNMR are 60.6 and 66.0 %, respectively.

4.2. Molecular weight, Solubility, Viscosity and thermal properties of B_3 and HBP.

Solubility results of HBP are compiled in Table 1S in supporting information. The solubility behavior of the polymer prepared in this study was determined in excess solvents at room temperature for 24 h. Molecular weight and molecular weight distribution of B_3 and HBP polymers were monitored by GPC technique. From the GPC technique, it is found that the average molecular weight of HBP (Mw 1363) is slightly higher in comparison to the molecular weight of B_3 (Mw 1181), because hydroxyl groups were incorporated into B_3, an increase of the M_W was expected. The viscosity is an important fluid property in order to study the rheological

behavior of polymers. Figure 5 illustrates viscosity (η) variation as a function of shear rate (γ) for four different temperatures 30, 40, 50, and 60 ^{o}C. The HBP shows Newtonian shear characteristics at variation of temperature ranging from 30-60 ^{o}C i.e. Viscosity is dependent on shear rate. As can be seen in Figure 5, HBP exhibited the same viscosity pattern over temperature, which was a non-linear decrease in viscosity with increasing temperature. The viscosities of HBP at different temperature with a shear rate of 23.3 s^{-1} are 30 ^{o}C, 0.843 Pa.S; 40 ^{o}C, 0.497 Pa.S; 50 ^{o}C, 0.224 Pa.S; and 60 ^{o}C, 0.122 Pa.S respectively. This temperature effect on samples viscosity has been attributed to decreased intermolecular interactions by great thermal molecular movement. The thermal transitions of B_3 and HBP like glass transition (-30.8 ^{o}C and -32.2 ^{o}C for B_3 and HBP respectively) were determined by DSC and shown in Figure 1S in supporting information. In order to study the influence of the chemical structure on the glass transition of a polymer, the phenomenon should be examined in these polymers. Generally, it is said that T_g directly proportional to average molecular weight of the polymer. In our case, results are consistent with this statement. The structural variation in the B_3 backbone due to introduce of the hydroxyl group with addition of GLY has affected glass temperature significantly. In addition, acid value and hydroxyl value of B_3 and HBP were measured from aforementioned ASTM standards and they were almost in consistent with the theoretical values (B_3: theoretical acid value – 429, experimental acid value – 420 and HBP: theoretical hydroxyl value – 547 and experimental hydroxyl value –535). Theoretical values for B_3 and HBP were calculated from their expected structures and also according to their mole ratio of reactants. TGA is used to measure a variety of polymeric phenomenon involving weight changes, sorption of gases, desorption of contaminant, and degradation. The thermal degradation study of B_3 and HBP were done in a N_2 environment at a heating rate of 10 ^{o}C/min. In the TGA thermograms for B_3 and

HBP, two-step decomposition profiles were observed as shown in Figure 6. The initial degradation of the B_3 might be attributed to loss of carboxylic groups whereas in the HBP is due to the degradation of peripheral glycerol moiety. It was noticed from the TGA profile that, the thermal stability of the B_3 is higher than the HBP. The main decomposition of the samples takes place in the second stage of degradation, i.e., above the temperature 370 ^oC. The values of T_{ON} (initial decomposition temperature for degradation step), T_{end} (final decomposition temperature for degradation step) and % weight remaining at 200 ^oC, 300 ^oC, 400 ^oC and 500 ^oC are summarized in Table 3.

4.3. FTIR analysis of PU films. The FTIR spectra of different HBPPU films are shown in Figure 2S in supporting information. The isocyanate terminated HBPPU prepolymer is characterized by FTIR spectroscopy, which shows the characteristic absorption band at 2270 cm^{-1} due to the existence of the isocyanate groups, was completely disappeared after moisture curing. Also, the characteristic bands of urethane stretching –N–H at 3500 cm^{-1}, a combination of urethane carbonyl –NH–CO–O and esteric carbonyl –CO–O at 1742 cm^{-1}, and a combination of –N–H out-of-plane bending and –C–N stretching at 1532 cm^{-1} present in the spectra. In addition to that, the disappearance of absorption bands at 3400 and 1412 cm^{-1} confirmed the absence of free hydroxyl groups in the HBPPU prepolymer films.

4.4. DMTA analysis. DMTA measures the deformation of a material in response to oscillating forces and this technique is used to detect the viscoelastic behavior of polymeric materials and yields quantitative results for the tensile storage modulus E′ and the corresponding loss modulus E″. The loss factor tan δ can then be expressed as the quotient of loss and storage, E″/E′. E′ and E″ characterize the elastic and viscous component of a material under deformation, E′ is a measure of the mechanical energy stored under load. The tan δ compares the amounts of

dissipated and stored energy. T_g values of the coating films are obtained from the peaks of tan δ curves. The E′ values in rubbery region at T >T_g are taken to calculate crosslink density (υ_e) by using Equation (2). [25,26]

$$\upsilon_e = E' / 3RT \qquad (2)$$

Where R is the universal gas constant, and T the temperature in K (T > T_g).

To observe the effect of NCO:OH ratio on dynamic mechanical properties, the E′ and tan δ temperature curves for the representative coating films are shown in Figure 7 and Figure 8 respectively, while the data is reported in Table 4. The T_g values of HBPPU-2, HBPPU-1.6, HBPPU-1.4 and HBPPU-1.2 are 124.9, 103.2, 97.76 and 95.56 ^oC, respectively. The E′ values of HBPPU-2, HBPPU-1.6, HBPPU-1.4 and HBPPU-1.2 coating films are 2.003 $\times 10^9$, 1.362$\times$ $10^{9,}$ 1.003$\times$ 10^9 and 1.479 $\times 10^8$, respectively at 40 ^oC. Usually, hard materials have a modulus of 10^9–10^{10} Pa and rubbery materials of 10^6 Pa.[27] This indicates the good mechanical integrity of coatings. The data suggests that the material stiffness, T_g, and crosslinked density of the HBPPU coatings increases with the increase in NCO/OH ratio. This may be due to the formation of more urethane/urea segments in the matrix with increasing NCO/OH ratio which restricts the chain mobility through hydrogen bonding.[28,29]

4.5. Chemical resistance: The percentage of weight loss of the PU films were calculated in sulphuric acid, hydrochloric acid, sodium hydroxide, sodium chloride, toluene, chloroform, methyl ethyl ketone and distilled water. The PU films were suspended in various chemical environments for 7 days and tested for change in weight and the corresponding data was furnished in Table 5.

4.6. TGA analysis. The thermal stability of HBPPU-2, HBPPU-1.6, HBPPU-1.4 and HBPPU-1.2 coating films was evaluated from the TGA data derived from the thermogravimetric

analysis in N_2 environment. TGA curves of the coating films are shown in Figure 9. The values of T_{ON} (initial decomposition temperature for degradation step), T_{max} (maximum decomposition temperature for degradation step), T_{end} (final decomposition temperature for degradation step) and % weight loss temperature at 20, 50 and 90% are summarized in Table 6. All the coating films show three steps degradation profile. The data in table show that the thermal stability of the coating films is increased with increasing the NCO:OH ratio. For instance, the maximum degradation temperature and 50% weight loss temperature for the coating films HBPPU-2, HBPPU-1.6, HBPPU-1.4 and HBPPU-1.2 are 311.5, 309.2, 308.9, 307.2 ^{o}C and 316.8,308,307.6,305.1 ^{o}C respectively. This trend indicates the formation of more cross-linked and hydrogen bonded structures at higher NCO/OH ratio. More crosslinking and hydrogen bonding brings the polymer backbones closer and thus reduces the molecular mobility and also increases the thermal stability. This behavior supports the increase in T_g of the samples with increase in NCO/OH ratio in DMTA analysis.[30,31]

4.7. DSC analysis. The glass transition (T_g) properties of coating films were studied by DSC; their results are displayed in Figure 10 and reported in Table 4. The glass transition temperatures of HBPPU-2, HBPPU-1.6, HBPPU-1.4 and HBPPU-1.2 coatings are 117.65, 92.08, 91.14 and 85.32 ^{o}C respectively. Generally, DMTA technique provides higher T_g values than DSC due to the dynamic nature of the test.[32] The glass transition temperature increases with increasing NCO:OH ratio, so it seems reasonable to assume that the mobility of organic polyurethane chains is greatly restricted by hydrogen bonding. The effect might be observed due to high cross-linking density of the films with increasing the cross-linker (IPDI), which restricted the segmental motion of the polymer chains and increased the glass transition temperature.

4.8. Contact angle. The hydrophobic natures of the HBPPU-2, HBPPU-1.6, HBPPU-1.4 and HBPPU-1.2 different coating films were evaluated by measuring the contact angle (CA). The water CA was in the range of 82^o - 78^o. The CA data of the coating films are HBPPU-2, 82.2^o; HBPPU-1.6, 81.3^o; HBPPU-1.4, 79.8^o and HBPPU-1.2, 78.1^o respectively. It can be confirmed that the improvement of the hydrophobic capacity of coating films by increasing NCO:OH ratio. The results show that, the higher CA observed for the formulation HBPPU-2 coating film among all other coating films.

4.9. XRD analysis. Figure 11 shows the X-ray diffraction curve of PU-urea the coating films. The X-ray diffraction pattern of PU-urea films depends on the NCO:OH ratios and alters the symmetry and regularity of the polymer matrix and therefore increasing its crystalline character. All diffractogrammes contain a broad peak around 18^o (2θ angle), which suggests that the diffraction is mostly by an amorphous polymer region. The higher broad peak is obtained in the HBPPU-1.2 sample, but the broad peak around 18^o whose intensities get decreased in the case of HBPPU-2. This might be due to the formation of more polar urea groups in the structure and formed more inter chain hydrogen bonding between the macromolecular chains which can induce disorganization.[33]

5. CONCLUSIONS

The present paper describes the synthesis of HBP based on Renewable resource in order to obtain a prepolymer with terminal hydroxyl groups and to develop poly(urethane-urea) coatings. For this purpose, the synthetic strategy (B_3+A_3) proposed here was convenient and effective for HBP synthesis to produce highly branched polyester polyol with the degree of branching almost equal to 66% that was further reacted with different ratios of isophorone diisocyanate to get an

isocyanate terminated polyurethane prepolymer. The excess isocyanate of the prepolymers was cured under atmospheric moisture to get polyurethane/urea coatings. B_3 and HBP were characterized by ^{1}HNMR, ^{13}CNMR, FTIR spectroscopy and thermal techniques. Coatings were studied for thermal, surface, and viscoelastic properties using different techniques. The coating property such as contact angle was also measured. Contact angle was directly dependent on the NCO:OH ratio. The hydrophobic character of the coating films was found to increase with an increasing NCO/OH ratio. The DMTA result suggests that the T_g and crosslink density of different HBPPU coatings increases with an increase in the NCO/OH ratios. The overall results will broaden the scope of coating formulator to design renewable based HBP polymers with thermally resistant and tough moisture curable coating composition with appropriate choice of NCO/OH ratio.

ACKNOWLEDGEMENTS

Somisetti Varaprasad and Shaik Allauddin would like to thank University Grants Commission (UGC) and Council of Scientific and Industrial Research (CSIR), New Delhi, India for the research fellowship. The present work was carried out under (CSC-0114) project.

REFERENCES

(1) K. K. Jena, K. V. S. N. Raju, B. Prathab and T. M. Aminabhavi, *J. Phys. Chem. B.,* 2007, **111**, 8801–8811.

(2) S. Kumari, A. Mishra, D. Chattopadhyay and K. V. S. N. Raju, *J. Polym. Sci. A Polym. Chem.,* 2007, **45**, 2673–2688.

(3) S. Kumari, A. Mishra, A. Krishna and K. V. S. N. Raju, *Prog. Org. Coat.,* 2007, **60**, 54–62.

(4) V. Wyatt, *J. Am. Oil Chem. Soc.,* 2011, **89**, 313–319.

(5) K. Inoue, *Prog. Polym. Sci.,* 2000**, 25**, 453–571.

(6) G. Jannerfeldt, L. Boogh and J. Månson, *Polymer***,** 2000, **41**, 7627–7634.

(7) D. K. Chattopadhyay and K. V. S. N. Raju, *Prog. Polym. Sci.,* 2007, **32**, 352–418.

(8) P. E. Froehling, *DYES PIGMENTS*, 2001, **48**, 187–195.

(9) Z. Wirpsza, *Polyurethanes: Chemistry, Technology and Applications,* Ellis Horwood, London, 1993.

(10) B. Bruchmann, R. Königer and H. Renz, *Macromol. Symp.,* 2002, **187**, 271–280.

(11) M. Jikei and M. Kakimoto, *Prog. Polym. Sci.,* 2001, **26**, 1233-1285.

(12) G. R. Newkome, C. N. Moorefield and F. Vo¨gtle, *Dendrimers and Dendrons: Concepts, Syntheses, Applications,* Wiley-VCH, Weinheim, 2001.

(13) J. Stumbé and B. Bruchmann, *Macromol. Rapid Commun.,* 2004, **25**, 921–924.

(14) P. J. Flory, *J. Am. Chem. Soc.,* 1952, **74**, 2718–2723.

(15) Q. Lin and T. Long, *Macromolecules,* 2003, **36**, 9809–9816.

(16) S. Unal, Q. Lin, T. Mourey and T. Long, *Macromolecules,* 2005, **38**, 3246–3254.

(17) J. Hao, M. Jikei and M. Kakimoto, *Macromol. Symp.*, 2003, **199**, 233–242.

(18) J. Hao, M. Jikei and M. Kakimoto, *Macromolecules,* 2002, **35**, 5372–5381.

(19) D. Yan and C. Gao, *Macromolecules,* 2000, **33**, 7693–7699.

(20) C. Gao and D. Yan, *Chem. Commun.*, 2001, 107-108.

(21) C. Gao and D. Yan, *Macromolecules,* 2001, **34**, 156–161.

(22) M. Carnahan and M. Grinstaff, *Macromolecules,* 2006, **39**, 609–616.

(23) V. Wyatt, G. Strahan and A. Nuñez, *J. Am. Oil Chem. Soc.,* 2010, **87**, 1359–1369.

(24) A. Kulshrestha, W. Gao and R. Gross, *Macromolecules,* 2005, **38**, 3193–3204.

(25) L. W. Hill, *J. Coat. Technol.,* 1992, **64**, 28-42.

(26) L. W. Hill, *Prog. Org. Coat.,* 1997, **31**, 235–243.

(27) R. Narayan and K. V. S. N. Raju, *Prog. Org. Coat.,* 2002, **45**, 59–67.

(28) J. Fu, L. Shi, S. Yuan, Q. Zhong, D. Zhang, Y. Chen and J. Wu, *Polym. Adv. Technol.,* 2008, **19**, 1597–1607.

(29) A. Mishra, S. Allauddin, K. R. Radhika, R. Narayan and K. V. S. N. Raju, *Polym. Adv. Technol.,* 2011, **22**, 882–890.

(30) S. Allauddin, R. Narayan and K. V. S. N. Raju, *ACS Sustain Chem Eng.,* 2013, **1**, 910–918.

(31) A. Asif and W. Shi, *Polym. Adv. Technol.,* 2004, **15**, 669–675.

(32) D. J. Martin, G. F. Meijs, G. M. Renwick, P. A. Gunatillake and S. J Mccarthy, *J. Appl. Polym. Sci.,* 1996, **60**, 557–571.

(33) P. Florian, K. K. Jena, S. Allauddin, R. Narayan and K. V. S. N. Raju, *Ind. Eng. Chem. Res.,* 2010, **49**, 4517–4527.

LIST OF TABLES

Table 1. Different formulations and mole ratios

Sample code	NCO:OH (IPDI)
HBPPU-2	2:1
HBPPU-1.6	1.6:1
HBPPU-1.4	1.4:1
HBPPU-1.2	1.2:1

Table 2. $^{1}H\&^{13}C$ NMR resonance assignments for different glycerol branching patterns

	DENDRITIC UNIT(D)	LINEAR UNIT(L)		TERMINAL UNIT(T)		Degree of branching (DB)%
		$L_{1,2}$	$L_{1,3}$	$T_{1,2}$	$T_{1,3}$	
H_a	4.23	4.21	4.04	4.03	3.53	
H_b	5.23	4.99	3.92	3.69	4.77	60.6
H_c	4.23	3.54	4.04	3.39	3.52	
C_a	62.08	62.49	65.16	65.93	59.75	
C_b	69.09	72.35	66.16	69.43	75.96	
C_c	62.08	59.45	65.16	62.88	59.75	66.0
C_x=O	171.66	171.91	171.91	172.03	-	
C_y=O	171.41	171.34	-	-	NA	
C_z=O	171.66	-	171.91	-	-	

Table 3. Thermal analysis data of B_3 and HBP

sample	T_{id} (^{o}C)	T_{max} (^{o}C)	T_{df} (^{o}C)	Weight percentage at			
				200 ^{o}C	300 ^{o}C	400 ^{o}C	500 ^{o}C
B_3	192.2	374.6	416.2	79.68	51.4	10.93	7.64
HBP	238.4	380.2	421.8	80.89	59.92	13.53	8.98

Table 4. DMTA data of PU films

Sample code	T_g (^oC, DSC)	T_g (^oC)	E′ at 40 ^oC [Pa]	Tan δ	E′ at T_g+5 ^oC [Pa]	υ_e (T_g+5 °C) (mole/cm^3)
HBPPU-2	117.65	124.9	2.003×10^9	0.7	5.131×10^7	$5.17\ 2\times\ 10^{-3}$
HBPPU-1.6	92.08	103.2	$1.362\times\ 10^9$	0.86	3.639×10^7	$3.88\times\ 10^{-3}$
HBPPU-1.4	91.14	97.76	$1.003\ \times10^9$	0.87	2.755×10^7	$2.98\times\ 10^{-3}$
HBPPU-1.2	85.32	95.56	$1.479\ \times10^8$	0.66	3.816×10^6	$4.153\times\ 10^{-4}$

Table 5. Chemical resistance (in percent weight loss) of the PU films

Chemical	HBPPU-2	HBPPU-1.6	HBPPU-1.4	HBPPU-1.2
25%H_2SO_4	1.660	1.665	1.749	1.875
25%HCl	1.421	1.477	1.652	1.639
10%NaoH	0.512	0.564	0.719	0.655
10%NaCl	0.575	0.650	0.865	1.094
MEK*	0.781	0.833	1.230	1.554
$CHCl_3$	2.658	2.718	2.701	2.662
Toluene	1.145	1.476	1.619	2.052
Water	1.734	1.660	0.860	0.653

Table 6. Thermal analysis data of PU films

Sample code	T_{id} (^oC)	T_{max} (^oC)	T_{df} (^oC)	Wt.% loss temperature		
				20%	50%	90%
HBBPU-1.2	257.8	307.2	417.2	273.0	305.1	368.6
HBBPU-1.4	262.0	308.9	429.0	274.4	307.6	371.5
HBBPU-1.6	267.2	309.2	436.8	275.8	308.0	381.5
HBBPU-2	272.9	311.5	438.5	281.8	316.8	384.5

LIST OF FIGURES

Figure 1: FTIR Spectra of the B_3 and HBP

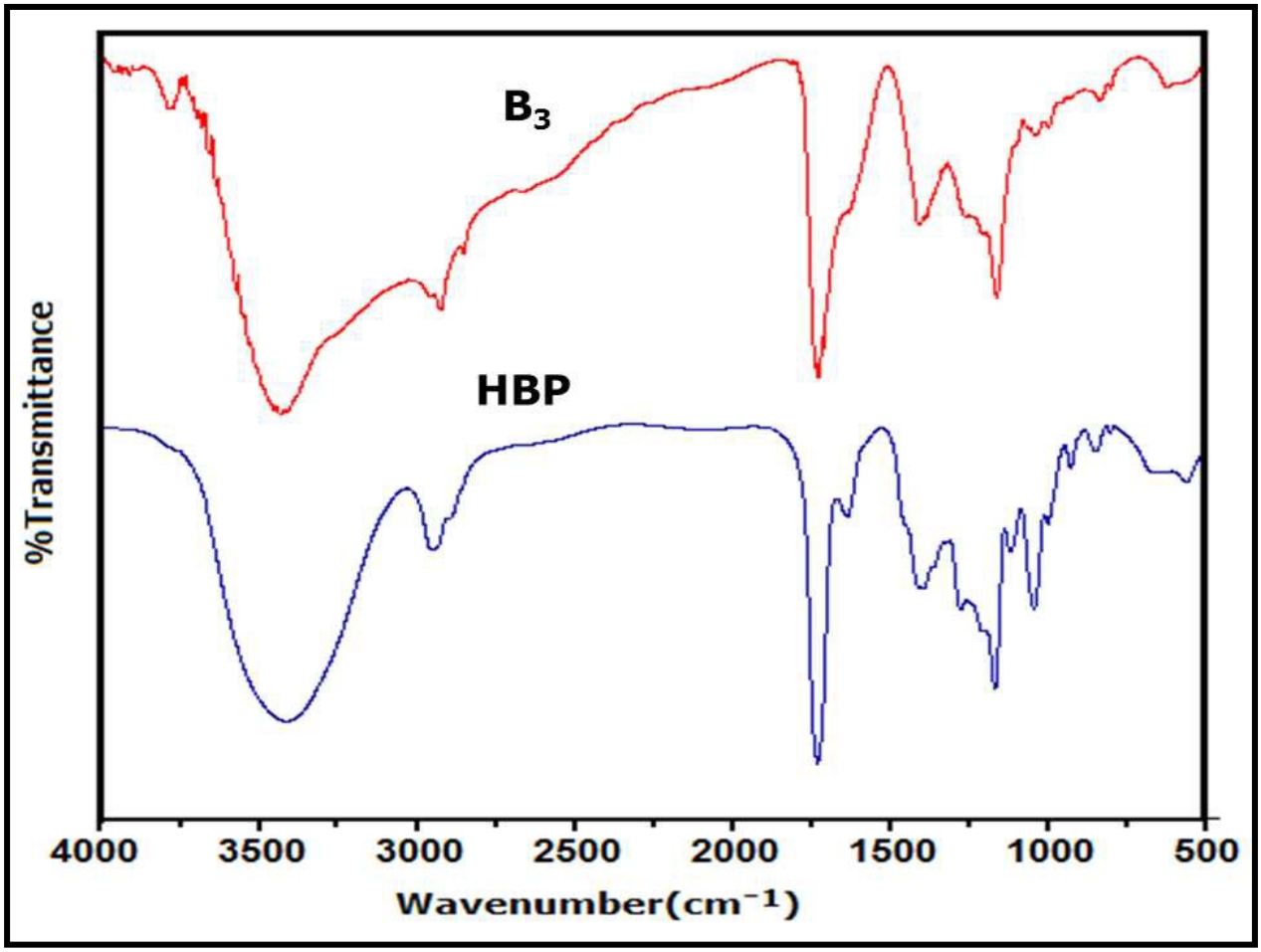

Figure 2. ^{1}HNMR spectra of B_3 & HBP

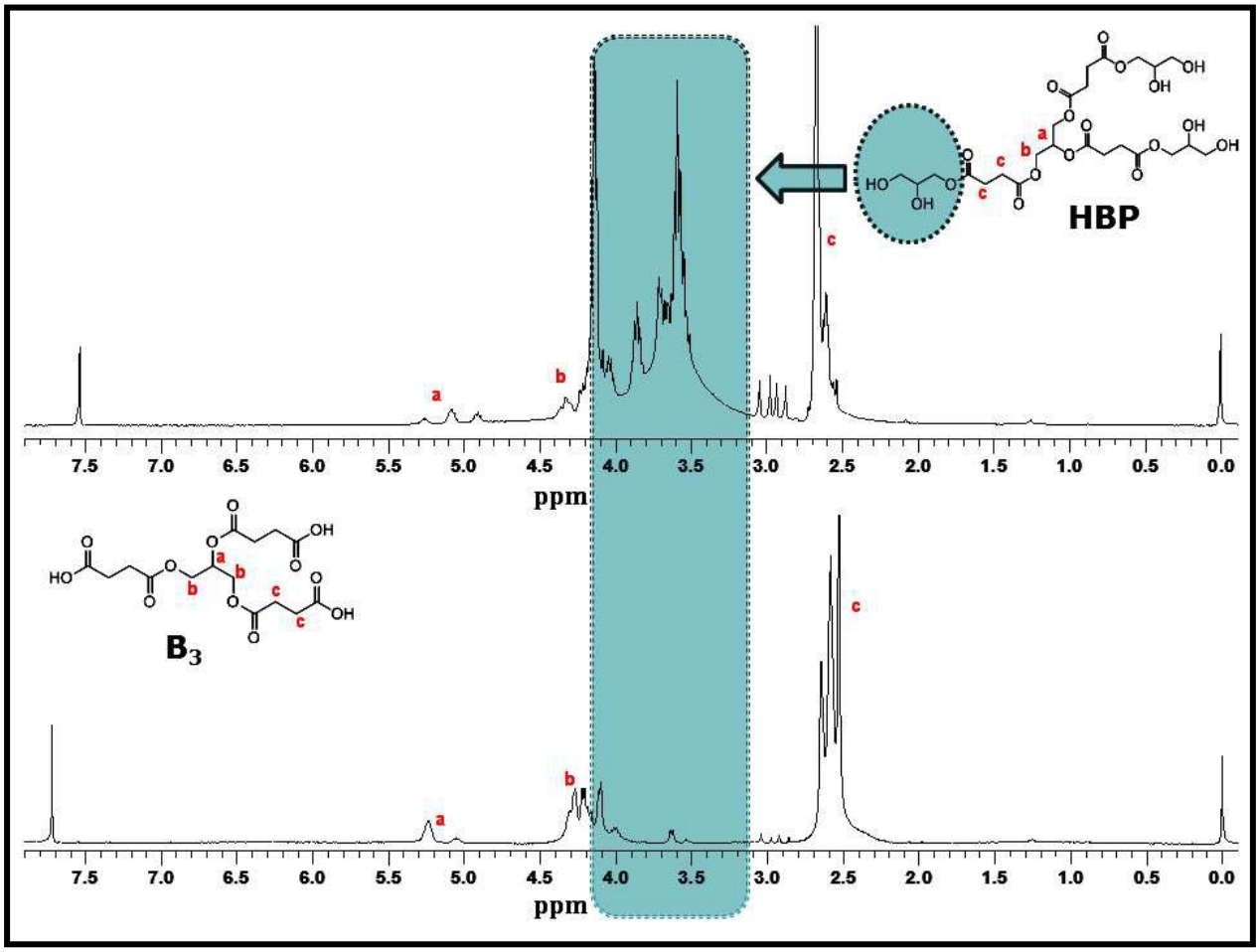

Figure 3. ^{13}CNMR spectra of B_3 & HBP

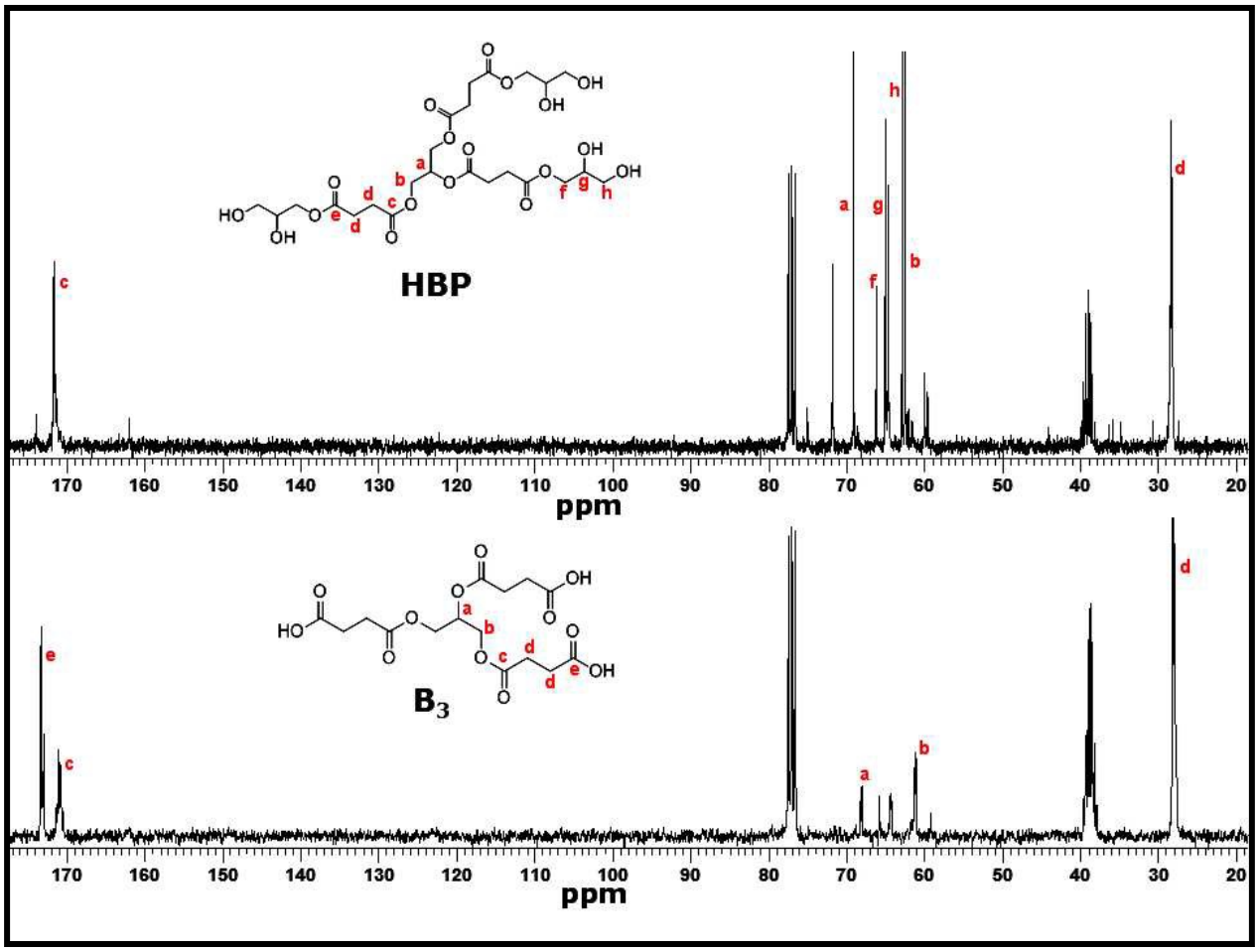

Figure 4. Degree of branching explanation by ^{1}H & ^{13}C NMR spectroscopy

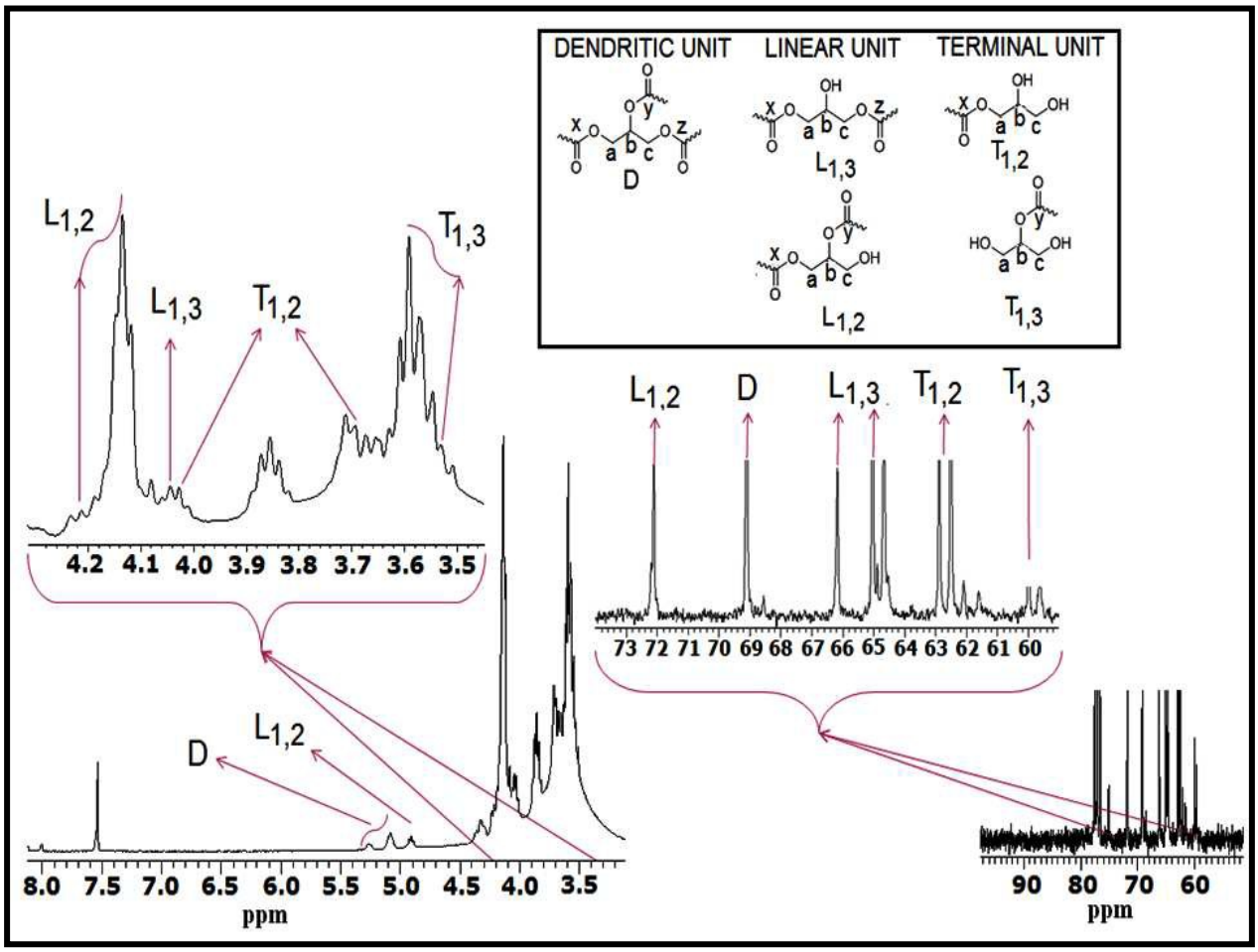

Figure 5.Rheology curves of HBP

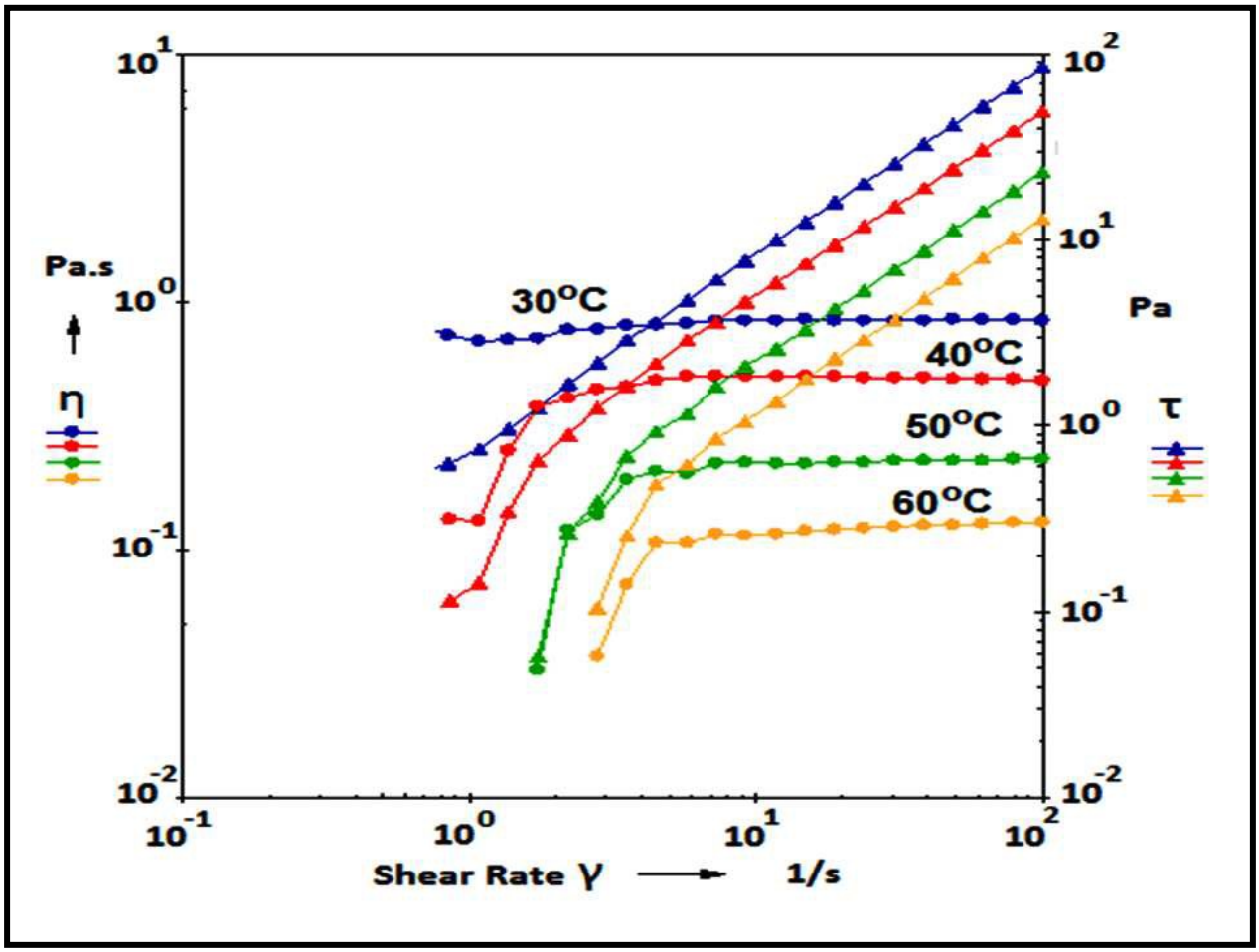

Figure 6. TGA curves of B_3 and HBP

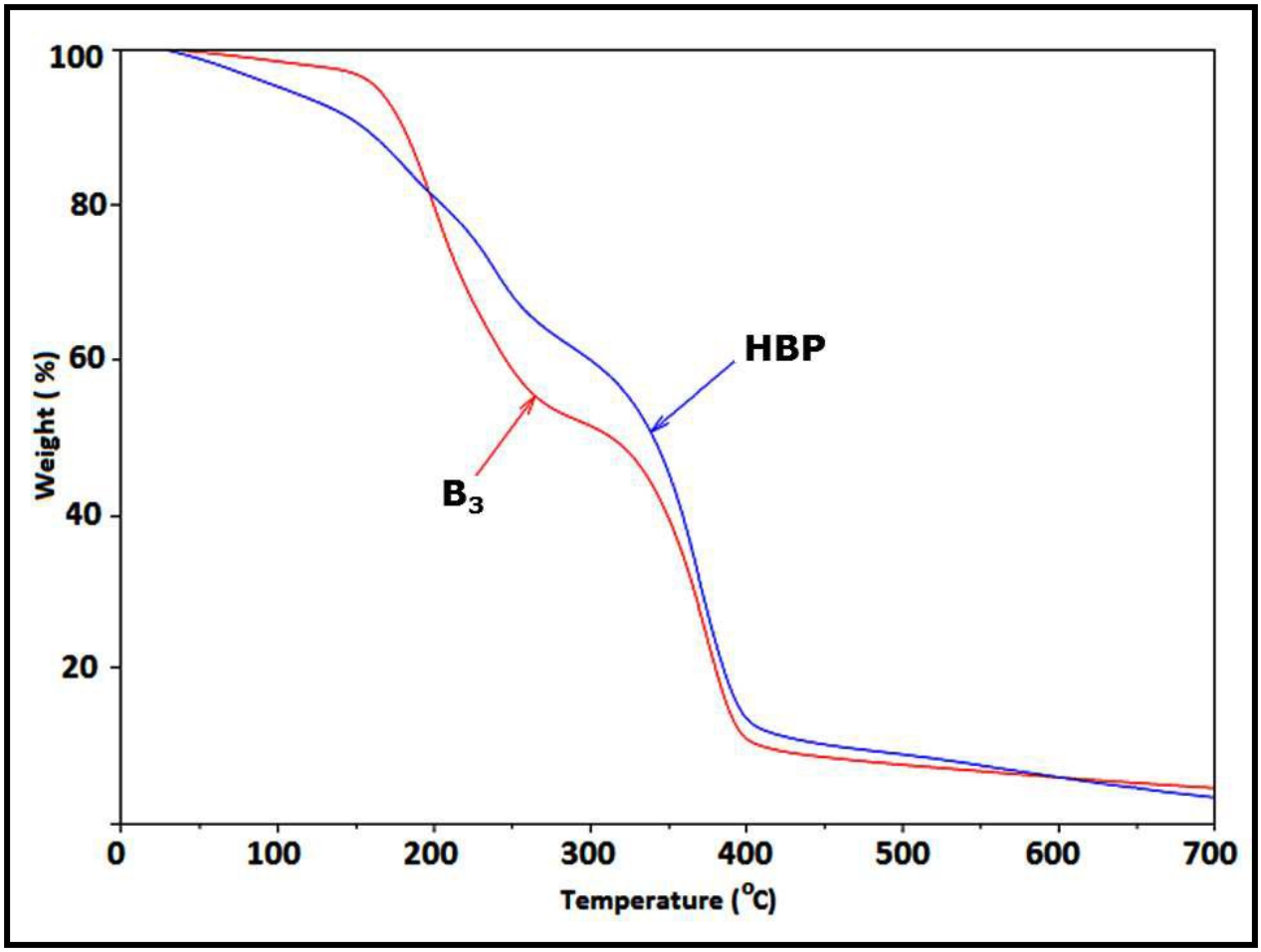

Figure 7. E' vs. temperature plot of the PU films

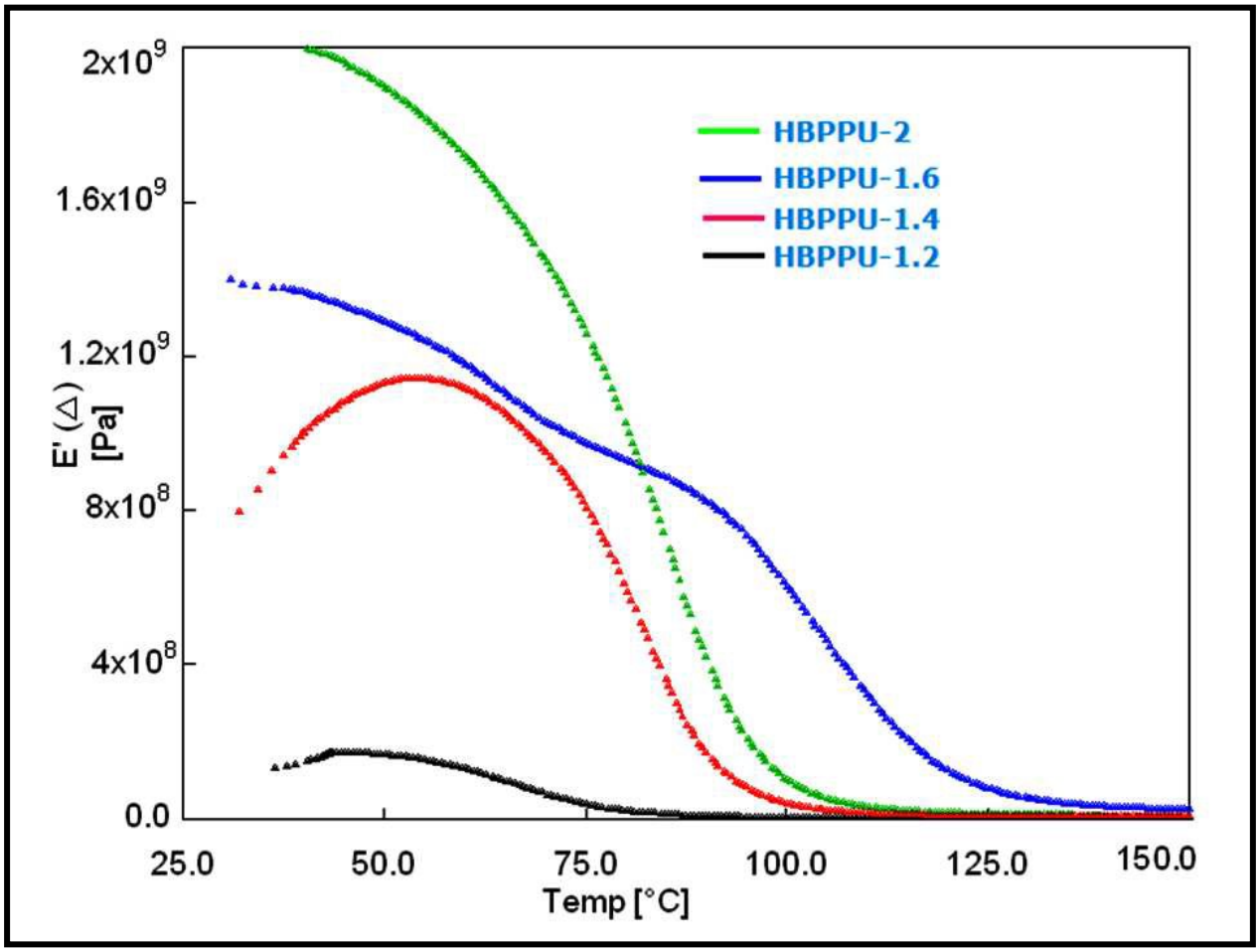

Figure 8. Tan δ vs. temperature plot of the PU films

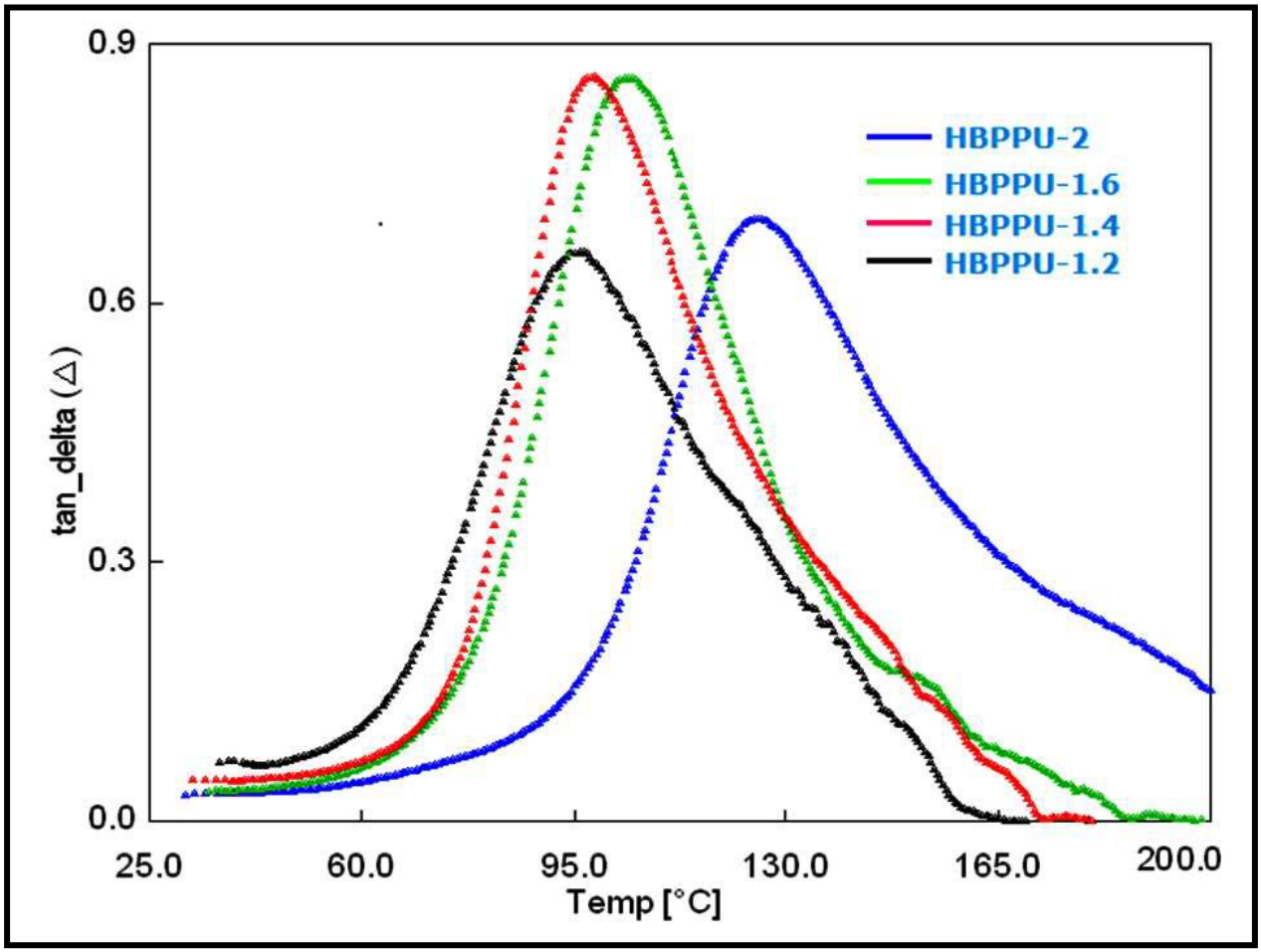

Figure 9. The TGA curves of PU films

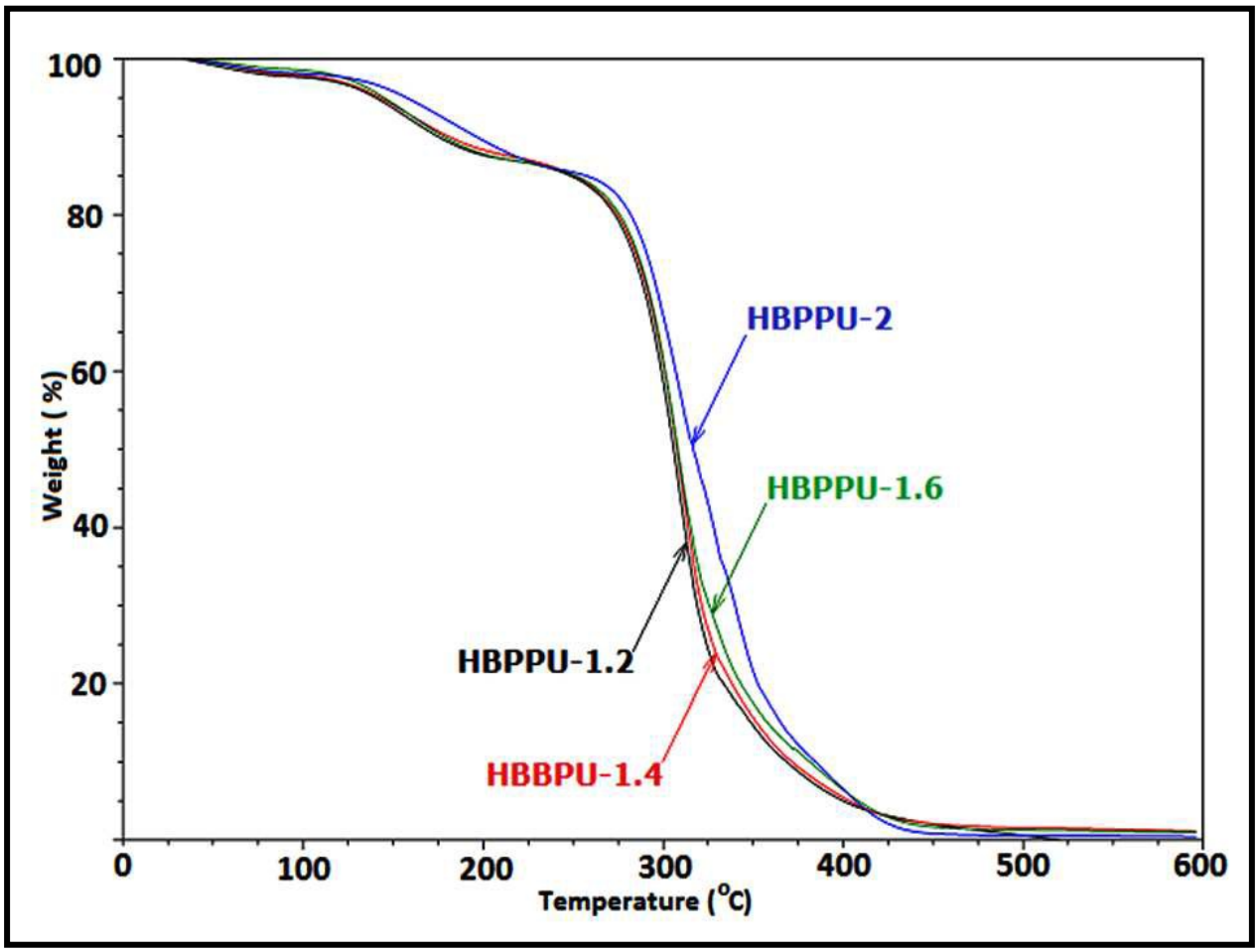

Figure 10. DSC curves of PU films

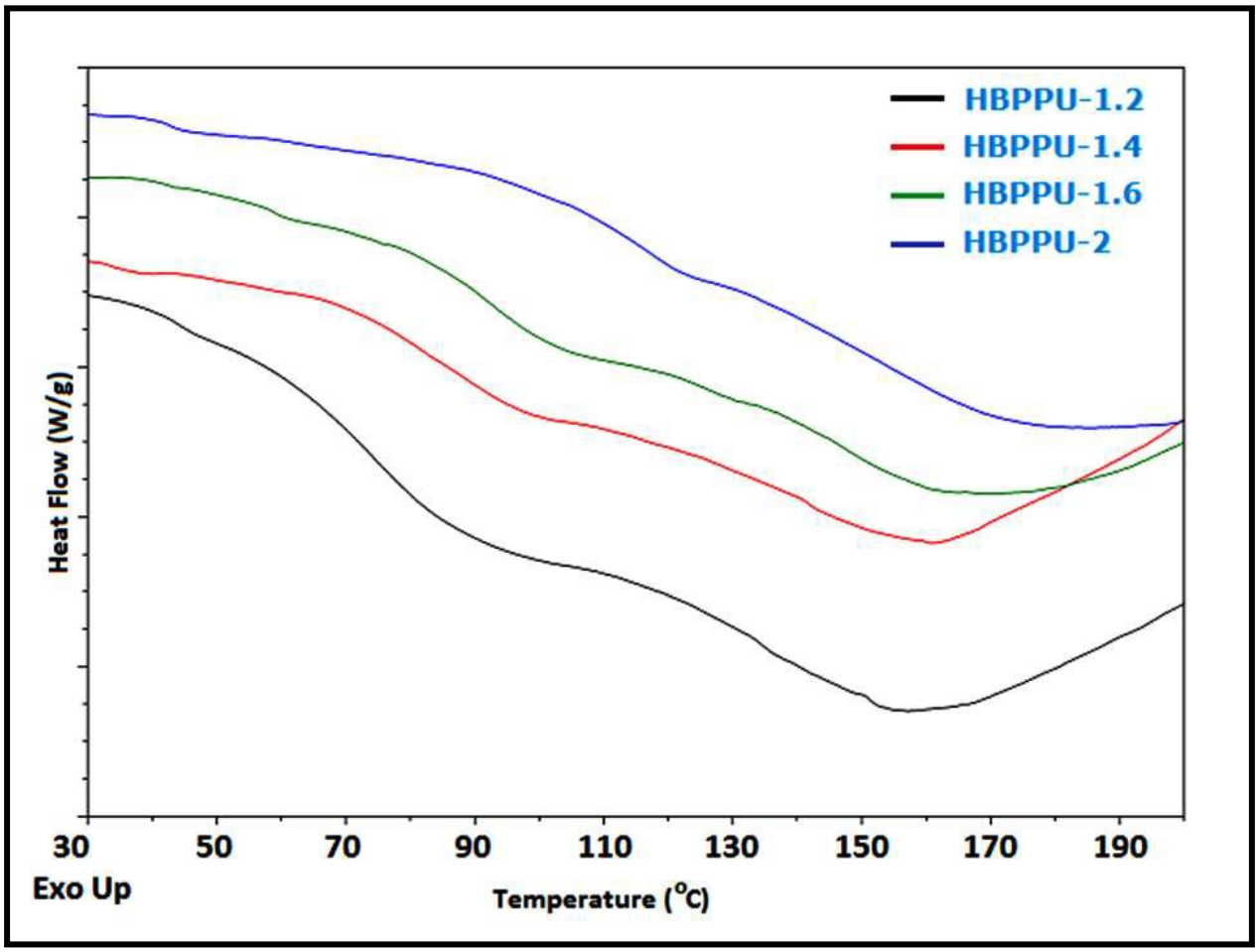

Figure 11. XRD of PU films

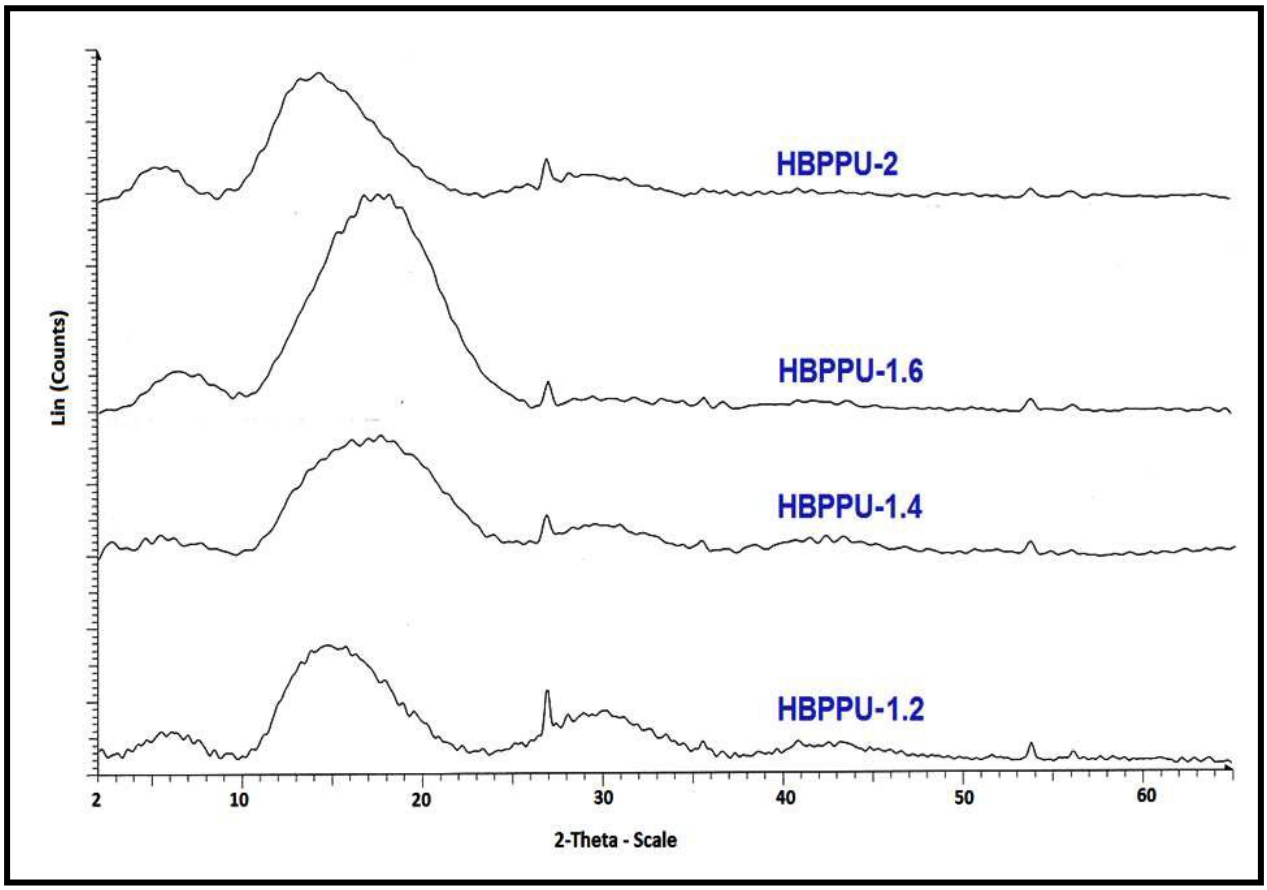

LIST OF SCHEMES

Scheme 1. Schematic representation of Synthesis of B_3 and HBP

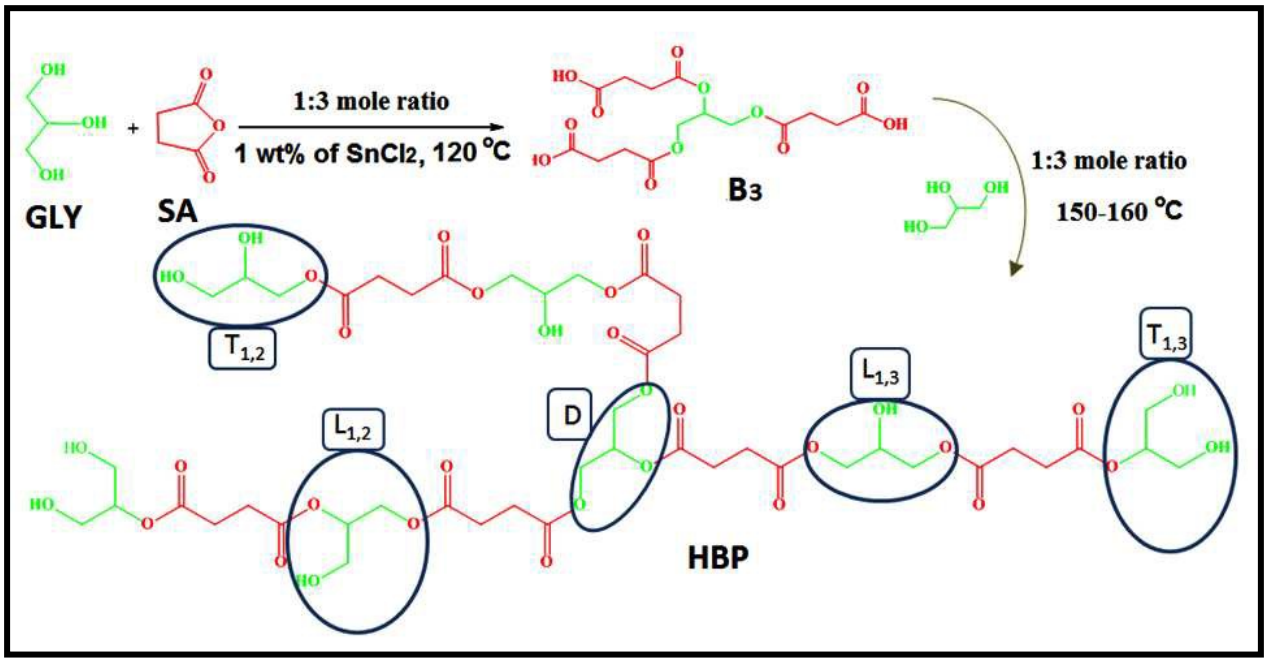

Scheme 2. Schematic representation for the formation of poly (urethane- urea) from HBP